Energy Recovery in Natural Gas Pressure Reduction Stations

Gonçalo Secca Serra
goncalo.secca.serra@tecnico.ulisboa.pt

Instituto Superior Técnico, Universidade de Lisboa, Portugal

June 2018

Abstract

High-pressure natural gas (NG), which flows through the Portuguese transmission system, is split into several branches before arriving to consumers. At the distribution network entrance, NG pressure must be reduced to reach day-to-day consumers needs (industrial or domestic purposes). These reductions occur through expansion valves lowering the pressure from 50-70 bar to nearly 20 bar. In a competitive global market, where environment concerns are paramount, energy waste is a key issue, which explains the current growing interest in recovering energy from the NG pressure reduction. A system with a turboexpander (TE) driving a generator is, therefore, suggested for the production of electrical energy. A thermodynamic analysis of the proposed system was made and several simulations were performed with a MATLAB model, showing that the energy recovery from this pressure drop is not as obvious as it seems. The reason is that the expansion cools the gas at temperatures that can cause hydrate formation. To avoid such drawbacks, some energy might have to be consumed to raise the temperature prior to expansion, which may turn out to be unattractive on thermodynamic grounds, but still worth considering based on economic arguments.

Keywords: Energy Recovery, Natural Gas, Expansion Turbine, Pressure Reduction.

1. Introduction

In a world highly dependent on fossil fuels, energy production is a major concern, leading to a daily search for new sources of renewable energy, as well as improvements in the efficiency of current systems. NG transport system, summarised in Figure 1, is an example where it may be possible to recover energy. Once extracted, the NG is processed and compressed before being injected, under high-pressure, into a transmission piping system. The standard pressure varies between 50 and 70 bar, however, to be delivered to distribution companies or power plants, the gas must be reduced close to 17 bar and 42 bar, respectively. The pressure reduction occurs in the so-called City Gate Station (CGS), through the use of pressure regulators.

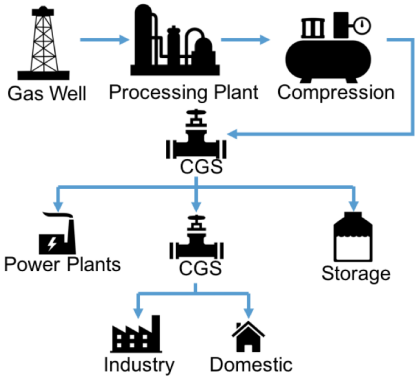

Figure 1: NG Transport Chain.

This process is nothing more than a simple expansion in a throttling valve, which, due to the Joule Thompson effect, slightly cools the NG. As a result, a heat exchanger (HX) coupled to a boiler is used to heat up the gas before expansion, avoiding low outlet temperatures that may cause condensation and hydrate formation. Since the huge pressure drop represents a decrease in the energy of the whole system, replacing the valve with a TE coupled to a generator may allow the recovery of some energy that would otherwise be lost. However, one should pay attention to the temperature drop, which is much higher than in a throttle valve, leading to higher heating requirements.

The aim of this research consists in evaluating several scenarios, where the aforementioned technology can be applied in Portugal. A thermodynamic analysis was made, giving some insight into the variables that most influence the feasibility of such systems.

2. Literature Review

The use of TE to produce electricity from the NG pressure reduction is not a recent idea. The concept has been explored, for CGS, since the 80's. One of the pioneer companies was San Diego Gas and Electricity, which in 1983 applied a TE to re-

duce the NG pressure from 55 to 26 bar. Without any heating, the electricity generated was about 890 MWh/year for the first 4 years of operation [1]. Leman and Worrell [2] mention three expansion turbine projects built in the 90's, one in Japan and two in the Netherlands. Regarding the latter, since 1991 there is a pressure reduction station which provides NG to the city of Amsterdam, using TE with the so-called Combined Heat and Power (CHP) technology. The heat supplied by the CHP units rises the gas temperature to more than 80°C, avoiding cooling below the critical temperature of hydrate formation, when the NG expands from 40 to 8 bar. In this facility, with an annual flow rate variation between 25,000 and 110,000 Nm^3/h, 12,022 MWh of electricity were generated in the first year, corresponding to a net power of 1.37 MW. The other Dutch project is located in the port city of IJmuiden. To heat the NG, waste heat from the refrigeration process of a nearby steel mill was used, instead of CHP units. Before the pressure reduction from 63 to 8 bar, hot water at 70°C rises the temperature of the NG. Throughout 1994, the system received 12,500 MWh of heat from the steel mill and generated roughly 11,000 MWh of electricity, with an average flow rate of 26 thousand Nm^3/h, which means that the system recovered almost 88% of the heat input. In Osaka, Japan, the scenario is quite different. The CGS is located near a district heating and cooling facility which supplies hot and cool water to the city. With a TE, the NG entering the station at an average temperature of 20°C, drops to -30°C. For this case, there is an opportunity to provide refrigeration energy to the cooling facility while the NG is heated up before being delivered to the distribution network. On the other hand, if there is little demand for cooling energy (e.g. during the winter), the NG can be heated before entering the turbine, using the waste heat generated by the heating facility. With an average flow rate of 15,000 Nm^3/h and a pressure reduction from 6 to 2 bar, in 1994 the TE generated 1400 MWh of electricity in 2600 hours [2]. In Bruxelles there is a 5.3 MW combined system running since 2002. With a nominal flow of 75,000 Nm^3/h, this CGS reduces the gas pressure from 14 to 1.7 bar. Lean-burned CHP units are used to produce 2.7 MW of electricity and to heat the gas at the TE inlet, which generates 2.6 MW [3]. Fuel cells are another promising technology. The fuel cell provides both electricity and heat without any combustion. In 2007, a TE and fuel cell integrated system started to work in Toronto, harvesting 2.2 MW (only 1 MW coming from the turbine) [4]. A summary of all the aforementioned cases is presented in table 1.

Several authors have been studying the benefits of TE pressure reduction systems in different countries. Software packages, such as HYSYS, are widely used in this type of simulations [5]. With these numerical tools, or simply with some thermodynamic calculations, the goal of all ongoing research is, basically, to gather data from a specific CGS in order to assess the economic relevance of energy recovery.

3. Actual System

In a standard CGS, once the NG enters, it is filtered to remove the dust and then it is heated. This temperature rise is necessary to avoid hydrate formation when the gas expands in a pressure regulating valve. Usually, there are two pressure reduction lines mounted in parallel, for reasons related to system maintenance and also to ensure a permanent supply of NG. A typical configuration of a CGS is shown in Figure 2.

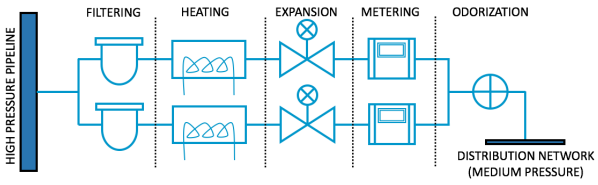

Figure 2: Typical configuration of a CGS [5]

The system is far from working in a steady-state regime, as shown in Figures 3 and 4, which present the time variation of pressure, temperature and flow rate at the inlet of two CGS , for industrial and domestic consumers [6].

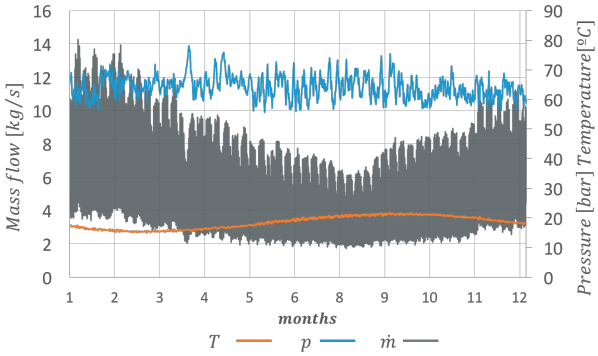

Figure 3: One year of records from a domestic CGS

Due to the fact that the pipelines are buried almost all the way, it is quite understandable that the temperature curve, observed in both figures, is similar to the soil temperature at 3 metres depth, whose values change between 13°C and 21°C [7]. Pressure evolution, on the other hand, seems to be much more random, which is related to viscous flow losses in pipe systems. The flow rate, on the contrary, is quite predictable. During winter, NG demand is higher than in summer months. However,

Table 1: Resume of some existing projects

Local		Year	Av.Flow $[\times 10^3 Nm^3/h]$	p_{in}/p_{out} $[bar]$	Heating	Power $[MW]$
San Diego, US	[1]	1983	-	55/26	none	0.1
Amsterdam, NL	[2]	1991	67.5	40/8	CHP and boilers	1.37
IJmuiden, NL	[2]	1994	26.5	63/8	Waste heat from a steel mill	1.26
Osaka, JP	[2]	1994	15	6/2	Heating and Cooling facility	0.54
Brussels, BE	[3]	2002	75	14/1.7	Lean burn CHP	2.6
Toronto, CA	[4]	2008	-	-	Fuel Cell and Boilers	1

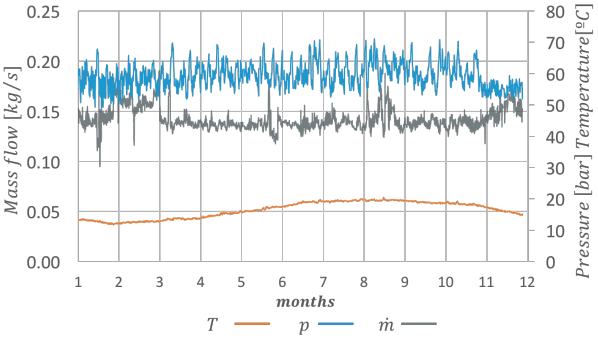

Figure 4: One of year records from an industrial CGS

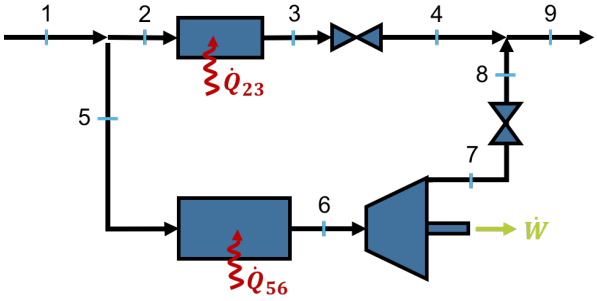

Figure 5: CGS scheme

in both winter and summer, the gap between the minimum and maximum values is quite large for domestic consumers as a result of peak consumption, whereas in the industrial sector this phenomenon is almost irrelevant, with only a slight increase during winter. The two main differences between domestic and industrial users are the pressure at the exit of the CGS and the order of magnitude of the flow rate. In the former case, outlet pressures are equal to 17 bar while in the latter a common value is 42 bar.

4. Proposed System

Scheme

Figure 5 depicts a standard configuration scheme of a CGS, when a TE is implemented to recover energy from the NG pressure reduction. The TE should be mounted in parallel to the existing line in order to guarantee normal operating conditions, in case the proposed system fails or requires maintenance. As the TE extracts energy from the NG, the temperature drop will be much higher than in a throttle valve. As a result, a HX coupled to a boiler must be placed before the expansion, just as in the original system. The temperature at the inlet of the TE is regulated by the HX. However, pressure may fluctuate at sections 6 and 7 and to ensure proper conditions at section 9 an expansion valve is placed after the TE.

Boundary Conditions

This system has some constraints that must be addressed. At a CGS, the NG arrives with a certain pressure, temperature and flow rate. These values,T_1, p_1 and $\dot{m}_1$, are imposed and fluctuate throughout the year as seen in Figures 3 and 4. When leaving the CGS, the NG must be at a pressure agreed with the consumers. Therefore, the outlet pressure is also a boundary condition. For each pressure, there is a threshold temperature below which hydrates can form. Hammerschmidt [8] proposed the following equation to calculate this minimum temperature:

$$T_{hf} = \frac{5}{9}(36.76(p \times 10^{-1})^{0.285} - 32) \qquad (1)$$

As a result, another constraint of the system is the minimum temperature at sections 8 and 4. Since it is assumed that $p_4 = p_8 = p_9$, this implies that $T_{4min} = T_{8min} = T_{9min}$. In summary, the boundary conditions are p_1, T_1, $\dot{m}_1$, p_9, with two constraints T_{4min} and T_{8min} and (subscripts refer to Figure 5).

Natural Gas

The NG is a complex mixture of hydrocarbons, extracted from underground sources. It is composed primarily by methane, but also includes ethane, propane and other hydrocarbons in smaller amounts. As shown in table 2, near 90% of the NG is methane. This is the reason why, in some studies and simulations, methane is often used to obtain approximate solutions. The same approach is followed in this study.

Table 2: Typical Composition of Natural Gas [9].

Name	Formula	Volume (%)
Methane	CH_4	>85
Ethane	C_2H_6	3 - 8
Propane	C_3H_8	1 - 2
Butane	C_4H_10	<1
Pentane	C_5H_12	<1
Carbon dioxide	CO_2	1 - 2
Hydrogen sulfide	H_2S	<1
Nitrogen	N_2	1 - 5
Helium	He	<0,5

Real vs Ideal Gas

To simplify the thermodynamic analysis, it is common to consider an ideal gas, described by a simple equation of state (EOS):

$$p = \rho RT \tag{2}$$

With this assumption and neglecting kinetical and potential energy variations, the generalized Bernoulli equation for an expansion valve becomes:

$$\frac{p_1}{\rho_1 g} + \frac{{v_1}^2}{2g} + z_1 + h_{f_{12}} = \frac{p_2}{\rho_2 g} + \frac{{v_2}^2}{2g} + z_2 \tag{3}$$

$$\Leftrightarrow h_{f_{12}} = \frac{p_1}{\rho_1 g} - \frac{p_2}{\rho_2 g} \tag{4}$$

$$\Leftrightarrow h_{f_{12}} = \frac{R(T_1 - T_2)}{g} \tag{5}$$

where $h_{f_{12}}$ is the head-loss in the valve. On the other hand, the energy balance of the valve, is given by:

$$\dot{m}(h_1 - h_2) = \dot{m}\bar{c}_p(T_1 - T_2) = 0 \tag{6}$$

where $\bar{c}_p$ is the mean specific heat, at constant pressure, between temperatures T_1 and T_2. From the previous equations one concludes that $\Delta T = 0$ and $h_{f_{12}} = 0$. Therefore, the ideal gas assumption leads to a contradiction and another EOS must be chosen.

For a pure substance the infinitesimal changes in internal specific energy and enthalpy are [10], respectively, equal to $du = c_v dT + (\partial u/\partial v)_T dv$ and $dh = c_p dT + (\partial h/\partial p)_T dp$. Since $(\partial u/\partial v)_T = T(\partial p/\partial T)_v - p$ and $(\partial h/\partial p)_T = v - T(\partial v/\partial T)_p$, integrating one obtains:

$$u_2 - u_1 = \int_1^2 c_v dT + \int_1^2 \left[T\left(\frac{\partial p}{\partial T}\right)_v - p \right] dv \tag{7}$$

$$h_2 - h_1 = \int_1^2 c_p dT + \int_1^2 \left[v - T\left(\frac{\partial v}{\partial T}\right)_p \right] dp \tag{8}$$

To compute equations 7 and 8, an EOS is required. There are several EOS and some of them are quite accurate at predicting the NG properties. As stated in [11], complex models, such as AGA and MGREG, are commonly used as well as Peng-Robinson, Redlich-Kwong-Soave and other cubic EOS.

To simplify the analysis, the Van der Waals (VdW) equation 9 was chosen. VdW EOS takes into account the volume occupied by the molecules (factor b) and the interactions between them (factor a). These two factors depend on the gas composition and are well-known [10].

$$p = \frac{RT}{v - b} - \frac{a}{v^2} \tag{9}$$

5. Mathematical Formulation

Heat Exchangers

Assuming an isobaric evolution in the HX, the energy balance yields:

$$\dot{Q} = \dot{m}\Delta h = \dot{m}\bar{c}_p \Delta T \tag{10}$$

Equation 8 requires knowledge of $v(T)$, which is not possible with VdW EOS. Therefore, the integration path between two generic states 1 and 2 is split into an isothermal path between 1 and x, followed by an isobaric path between x and 2 (Figure 6).

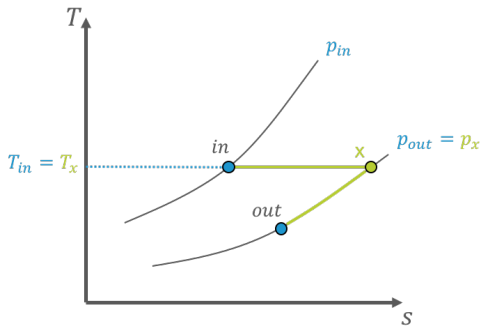

Figure 6: path on T-s diagram

Having said that, the first term of equation (7) disappears from 1 to x, and in equation (8) only the first term needs to be calculated from x to 2. Bearing this in mind, equations (11) and (13) are obtained:

$$u_x - u_1 = a\left(\frac{1}{v_1} - \frac{1}{v_x}\right) \tag{11}$$

$$h_x - h_1 = (u_x - u_1) + (p_x v_x - p_1 v_1) \tag{12}$$

$$h_2 - h_x = \bar{c}_p\,(T_2 - T_x) \tag{13}$$

Equation (12) comes from the definition of enthalpy. Summing the two enthalpy changes, yields a general equation for Δh:

$$h_2 - h_1 = a\left(\frac{1}{v_1} - \frac{1}{v_x}\right) + (p_x v_x - p_1 v_1) + \bar{c}_p\,(T_2 - T_x) \tag{14}$$

The value of $\bar{c}_p$ is an average value between states 2 and x, taken from a superheated methane table [12].

Expansion Valves

In expansion valves the energy balance implies that $\Delta h = 0$ [10]. Then, using equation (14), the outlet or inlet temperature can be obtained knowing the pressure on both sides and one of the temperatures. For T_{out} the equation is:

$$h_{in} - h_{out} = 0 \Leftrightarrow T_{out} = T_{in} - \frac{a}{\bar{c}_p}\left(\frac{1}{v_{in}} - \frac{1}{v_x}\right) - \frac{1}{\bar{c}_p}\left(p_{out}v_x - p_{in}v_{in}\right) \quad (15)$$

Where the 2^{nd} and 3^{rd} term are related to the real gas behaviour and make the temperature decrease in the valve.

Turboexpander

Once the turbine pressure ratio is set, the outlet pressure at the TE is calculated from the inlet pressure, which is equal to the pressure at the entrance of the CGS, neglecting viscous dissipation in the HX and pipes. As a result, the unknown variable in TE is the inlet temperature T_6. Figure 7 shows the relevant points to find the solution.

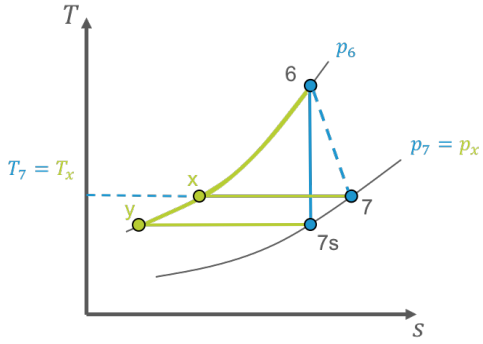

Figure 7: path on T-s diagram

Two important equations to get T_6 are the entropy balance for an ideal TE (equation (16)) and the definition of isentropic efficiency (equation (17)).

$$\Delta s_{6-7s} = \int_6^{7s} \frac{c_v}{T}dT + \int_6^{7s}\left(\frac{\partial p}{\partial T}\right)_v dv = 0 \Leftrightarrow \frac{T_6}{T_{7s}} = \left(\frac{v_{7s} - b}{v_6 - b}\right)^{\frac{R}{\bar{c}_v}} \quad (16)$$

$$\eta = \frac{h_6 - h_7}{h_6 - h_{7s}} = \frac{a\left(\frac{1}{v_7} - \frac{1}{v_x}\right) + \left(p_x v_x - p_7 v_7\right) + \bar{c}_p\left(T_6 - T_x\right)}{a\left(\frac{1}{v_{7s}} - \frac{1}{v_y}\right) + \left(p_y v_y - p_{7s} v_{7s}\right) + \bar{c}_p\left(T_6 - T_y\right)} \quad (17)$$

With the VdW EOS for points 6, $7s$ and y, a system of 5 equations with 5 unknowns (T_6, T_{7s}, v_6, v_{7s} and v_y) is obtained and solved by an iterative method, outlined in Figure 8.

$$p_6 = \left(\frac{RT_6}{v_6 - b}\right) - \frac{a}{v_6^2} \quad (18)$$

$$p_{7s} = \left(\frac{RT_{7s}}{v_{7s} - b}\right) - \frac{a}{v_{7s}^2} \quad (19)$$

$$p_y = \left(\frac{RT_y}{v_y - b}\right) - \frac{a}{v_y^2} \Leftrightarrow p_6 = \left(\frac{RT_{7s}}{v_y - b}\right) - \frac{a}{v_y^2} \quad (20)$$

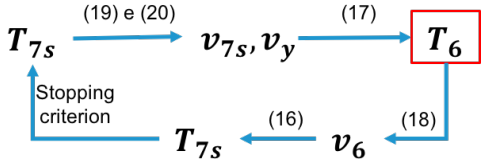

Figure 8: iterative process

If the temperature at the inlet of the TE is imposed, the computation of the outlet temperature requires only equations (16) and (17) to estimate the values of T_7 and T_{7s}, respectively. In addition, the work produced by the turbine is given by the equation:

$$\dot{W} = \dot{m}\left(h_6 - h_7\right) \quad (21)$$

In equation (17), TE's efficiency must be known. The large mass flow fluctuations over the year, or during a day, have an influence on TE's efficiency. Figure 9 depicts this dependence.

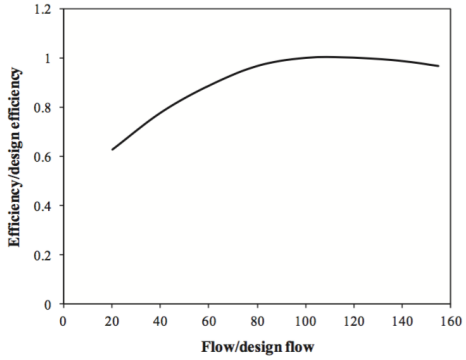

Figure 9: Relation between efficiency and flow [13]

Turboexpander Design

Since TE can withstand a mass flow of 20% to 150% of the design mass flow $\dot{m}_{des}$ [13], the value chosen is given by $\dot{m}_{des} = \dot{m}_{1max}/1.5$, where $\dot{m}_{1max}$ is the maximum mass flow at point 1. For industrial CGS $\dot{m}_1 > 0.2\dot{m}_{des}$ for all entry mass flows, which implies that the NG flows always through the TE, a situation that does not apply to domestic CGS. Regarding the design pressure ratio, it is defined by the ratio between the lowest inlet pressure recorded over the year (55 bar and 49 bar for the domestic and industrial CGS, respectively) and the outlet pressure. According to this definition, for the domestic CGS the pressure ratio yields 3.235, whereas it is equal to 1.167 for the industrial one. The design outlet temperature is calculated by equation (1), for an outlet pressure equal to 17 bar and 42 bar (domestic and industrial CGS, respectively). Moreover, the inlet design temperature is computed by the iterative method outlined in the previous section, assuming an initial efficiency of 80%. Radial flow TE are commonly used in this type of applications [1]. Two important equations have to be taken into account to compute the design efficiency:

$$N_s = \frac{0.076N\sqrt{\dot{V}}}{(\Delta h_i)^{\frac{3}{4}}} \tag{22}$$

$$SP = 1.49\dot{m}_1 \Delta h_i \eta_0 \tag{23}$$

where Δh_i (kJ/kg) is the ideal enthalpy difference between inlet and outlet, N (rpm) and N_s are the real and specific shaft speed, respectively, SP (kW) the estimated shaft power, $\dot{m}_1$ (kg/s) the mass flow, η_0 the initial estimation of the efficiency and $\dot{V}$ (m3/s) the exhaust volume flow. Once the shaft power is estimated, the rotational shaft speed can be taken from Figure 10, which relates SP with N [14].

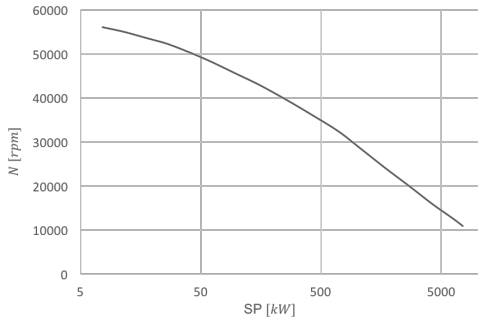

Figure 10: Relation between N and SP [14]

The specific rotational speed is computed with equation (22) and, finally, the design efficiency is obtained from Figure 11 for a radial TE.

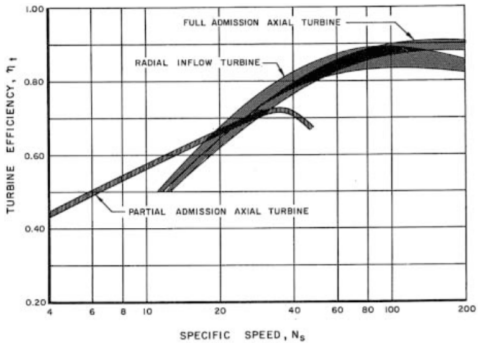

Figure 11: Relation between η_{des} and N_s [1]

6. Simulations

Five simulations were performed in order to analyse several variables that affect the system performance.

1^{st} - 1 year of operation

The purpose of this simulation is to evaluate how much energy can be recovered during one year. The input variables are the design conditions of the TE (η_{des}, PR and $\dot{m}_{des}$), the station's outlet pressure (p_9) and the NG state at section 1 (p_1, T_1 and $\dot{m}_1$), which can fluctuate throughout the year. To spare computational time, the MATLAB model was run with average monthly values of p_1, T_1 and $\dot{m}_1$. Furthermore, an average of the minimum and maximum values was obtained to gain insight into the capabilities of the system.

2^{nd} - Outlet Pressure

This second simulation aims at understanding the importance of p_9, which changes from domestic to industrial CGS. In this case, the values of p_1, T_1 and $\dot{m}_1$ are kept fixed as well as the design conditions (η_{des} and $\dot{m}_{des}$), with the exception of the PR, which depends on p_9.

3^{rd} - Heating Input

To investigate whether it is worth providing more heat than the required minimum, the value of T_{8min} was changed, which is tantamount to changing the heat input $\dot{Q}_{56}$, keeping constant p_1, T_1, $\dot{m}_1$, p_9 as well as the design conditions (η_{des}, PR and $\dot{m}_{des}$).

4^{th} - Design Efficiency

This simulation answers a basic question: if there is a decrease in heat supplied, what happens if the efficiency of the TE is improved? The design conditions were kept constant ($\dot{m}_{des}$ and PR) except for the design efficiency, which varies between 0 and 90%. The values of p_1, T_1, $\dot{m}_1$ and p_9 do not change either.

5^{th} - TE Inlet Pressure

As mentioned above, heating is required before the NG expands in the TE, in order to avoid hydrate formation. The goal of this simulation is to understand how the change in the inlet pressure of the TE affects the performance of the system, still ensuring that there are no hydrates. To control p_6 an expansion valve was placed just before the HX, thus reducing the pressure and temperature drop in the TE. The variables p_1, T_1, $\dot{m}_1$, p_9, η_{des} and $\dot{m}_{des}$ were kept constant. In this simulation, the TE line starts only after the HX of the other line, in order to maintain the temperature above hydrate formation after the new valve.

7. Results and Discussion

Figures 12 and 13 show, for domestic and industrial CGS, respectively, typical operation values obtained for a hour of the year. The inputs are in red.

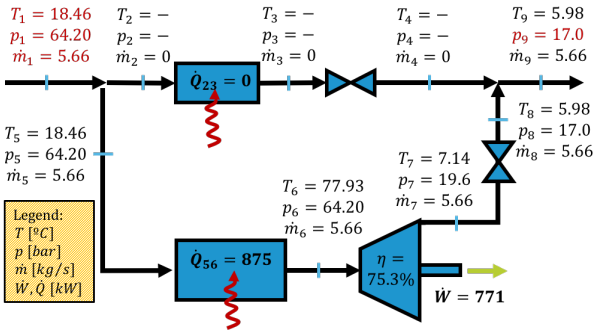

Figure 12: Results of a simulation in domestic CGS

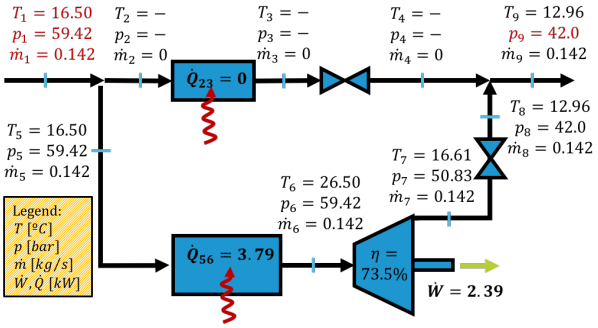

Figure 13: Results of a simulation in industrial CGS

Figure 14 shows the results of a one-year simulation, for an industrial CGS, assuming minimum inlet values. The curves of the work and mass flow are almost parallel, showing the strong dependence of $\dot{W}$ on $\dot{m}_1$. On the other hand, the heat $\dot{Q}_{56}$ depends mainly on the inlet temperature T_1 rather than $\dot{m}_1$. During the summer months, when T_1 is higher, decreases and the global efficiency increases, reaching values greater than 100%. Table 3 presents the values of the electrical energy produced over one year by both CGS. From these results one concludes that the annual energy recovered from a domestic CGS covers the energy needs of nearly 2800 typical residential dwellings in Portugal [15]. The values of the global efficiency η_{global} were computed dividing the work done by the heat supplied.

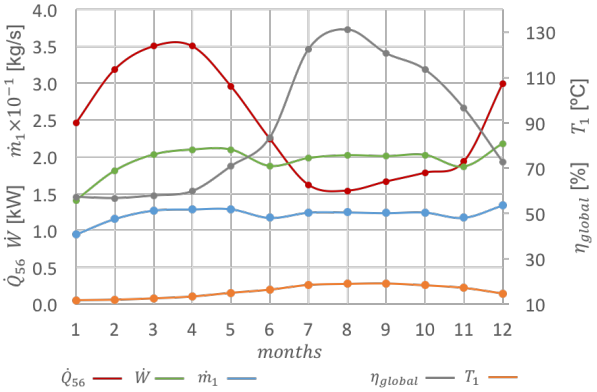

Figure 14: Variables along a year of an industrial CGS. $\dot{Q}$ and $\dot{W}$ have to be read on the left axis and all other variables on the right axis

Table 3: Values, in MWh, of the energy produced in both CGS.

	Domestic CGS			Industrial CGS		
	$\dot{W}$	$\dot{Q}$	η_{glob}	$\dot{W}$	$\dot{Q}$	η_{glob}
min	2167	1779	84	17	21	87
med	6803	7824	88	21	33	66
max	13,463	16,219	84	25	51	51

The main differences between both types of CGS are the outlet pressure and the magnitude of the mass flow. The values of $\dot{Q}_{56}$ and $\dot{W}$ depend directly on the mass flow $\dot{m}_1$, but the oulet pressure p_9 also affects them, as can be seen in figure 15 for the domestic CGS.

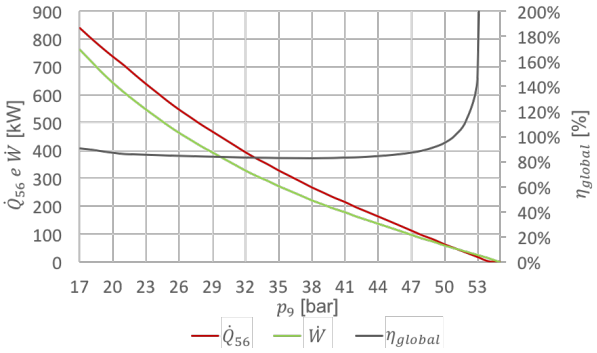

Figure 15: p_9 varying. $\dot{Q}$ and $\dot{W}$ have to be read on the left axis and all other variables on the right axis

Both $\dot{Q}_{56}$ and $\dot{W}$ decrease with increasing p_9 and, above a certain threshold ($p_9 \approx 51$ bar), $\dot{Q}_{56}$ becomes smaller than $\dot{W}$ which implies a sharp increase in global efficiency η_{global}. With the help of figure 16 the explanation of this phenomenon is quite straightforward. The orange line represents the temperature of hydrate formation in the p-h diagram. Since 9 must lie on this curve increasing p_9 implies a decrease in the enthalpy h_9, which may become smaller than h_1. Taking into account the energy balance $\dot{Q}_{56} - \dot{W} = \dot{m}_1(h_9 - h_1)$, one concludes that whenever $h_1 > h_9$ there is a net energy output, i.e., $\dot{W} > \dot{Q}_{56}$.

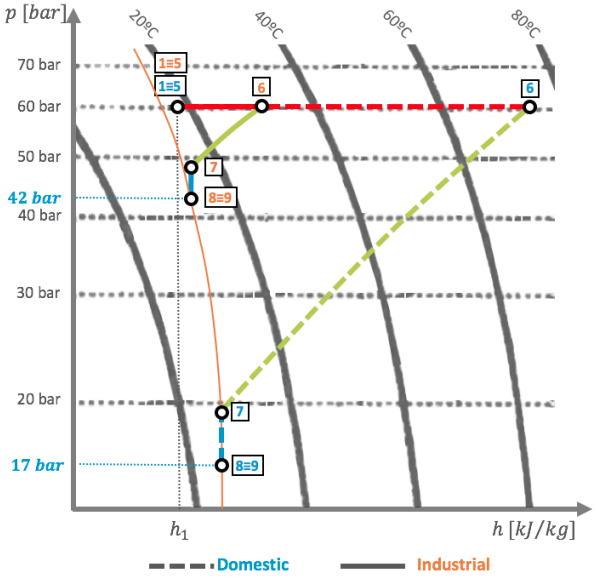

Figure 16: p-h diagram for domestic (blue) and industrial (orange) CGS

Figure 16 also compares the domestic and industrial CGS. In the former case $h_9 > h1$ and no energy can ever be recovered from the expansion, whereas in the latter case this possibility cannot be ruled out, as was already mentioned. This figure also shows that increasing p_9 the enthalpy change $h_6 - h_7$ along the turbine decreases, i.e., $\dot{W}$ decreases.

Regarding the third simulation, one might wonder whether the increase of T_{8min} has a relevant impact on the value of $\dot{W}$. Figure 17 shows that it has not, since $\dot{W}$ increases slightly compared to $\dot{Q}_{56}$, which implies a significant decrease in the global efficiency.

The fourth simulation is about the influence of the TE efficiency η_{des}. From Figure 18 it is possible to observe an increase in the values of $\dot{Q}_{56}$ and $\dot{W}$ with η_{des}. Global efficiency increases as well, but there is a tendency to saturation.

Finally, the results of the last simulation (Figure 19) show that the heating requirements can be significantly reduced by placing an expansion valve

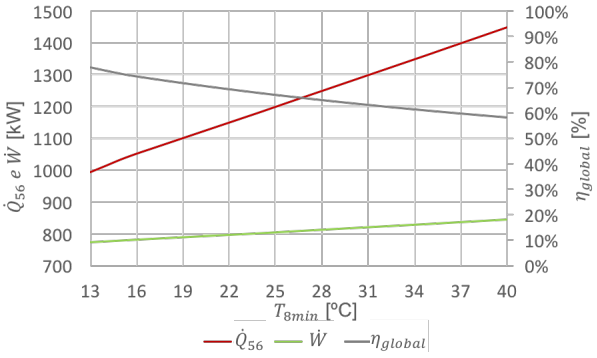

Figure 17: T_{8min} varying. $\dot{Q}$ and $\dot{W}$ have to be read on the left axis and η_{global} on the right axis

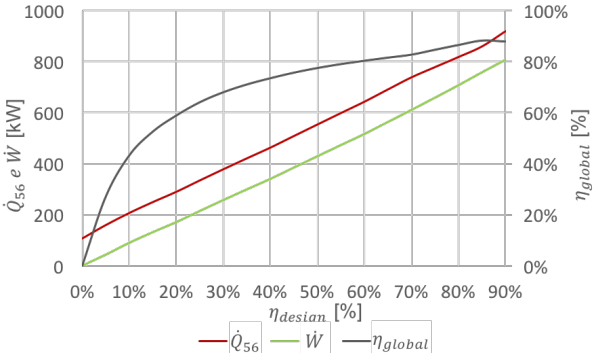

Figure 18: η_{design} varying. $\dot{Q}$ and $\dot{W}$ have to be read on the left axis and η_{global} and T_6 on the right axis

just before the HX. As a result, the pressure ratio in the TE decreases as well as $\dot{W}$ and $\dot{Q}_{56}$. However, there is a constraint imposed by the temperature of hydrate formation which is reflected on the increase of $\dot{Q}_{12}$. Figure 19 shows that, despite this, the total heat $\dot{Q}_{tot}$ decreases.

8. Exergy Analisys

In order to check the how the system is availing the potential to produce energy, an exergetic analysis was made. Assuming steady-state the exergy balance becomes:

$$\iint \dot{q}\left(1 - \frac{T_0}{T_q}\right) dA - \left(\dot{W} - p_0 \frac{dV}{dt}\right) - \dot{E}_d = \cancel{\frac{d}{dt}\iiint e\rho dV} + \iint e_f \rho(\vec{v} \cdot \vec{n}) dA \quad (24)$$

The scheme in Figure 20 shows the exergy that comes in and out of the proposed system. The exergy transferred from the boiler together with the exergy accompanying the fluid in 5 preform the total exergy that enters into the system. On the other hand, there is work generated and exergy accompanying the fluid that is leaving the system, which are, together with the losses by radiation and through the escape gases, the exergy outputs. Equation

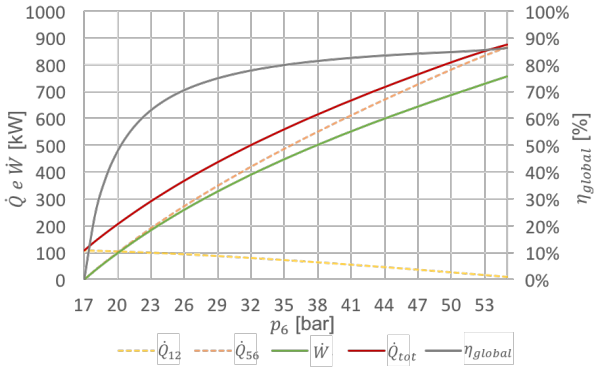

Figure 19: p_6 varying. $\dot{Q}$ and $\dot{W}$ have to be read on the right axis and all other variables on the left axis

(25), from exergy balance, shows clearly how each term contributes to the system, placing the inputs on the left-hand side and the distribution of this exergy on the right-hand side.

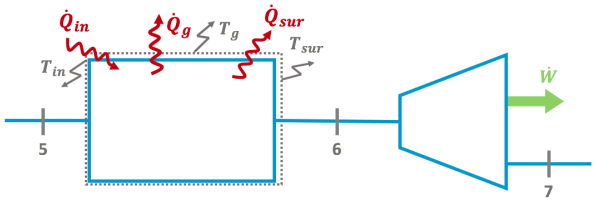

Figure 20: Proposed scheme exergy contributions.

$$\dot{Q}_{in}\left(1-\frac{T_0}{T_{in}}\right)+\dot{m}_5 e_{f_5}=\dot{W}+\dot{m}_7 e_{f_7}+ \dot{Q}_g\left(1-\frac{T_0}{T_g}\right)+\dot{Q}_{sur}\left(1-\frac{T_0}{T_{sur}}\right)+\dot{E}_d \quad (25)$$

In equation (25) the term $\dot{E}_d$ refers to the exergy that is destructed in the system, and is a sum of the rate of exergy destruction both in the boiler and in the TE ($\dot{E}_d = \dot{E}_{db} + \dot{E}_{dt}$).

Since the objective of the system is deliver NG to distribution network at a certain pressure and temperature at the same time that work is produced, the exergetic efficiency can be defined by equation (26), where this exergy outputs are divided by the exergy that comes into the system (boiler heat transfer and exergy accompanying entry gas).

$$\varepsilon=\frac{\dot{W}+\dot{m}_7 e_{f_7}}{\dot{Q}_{in}\left(1-\frac{T_0}{T_{in}}\right)+\dot{m}_5 e_{f_5}} \quad (26)$$

Having this, an exergy balance sheet was created in table 4, where can be observed that the most of the exergy that enters the system leave with the outlet flow, which maintain an huge potential of improvement. Assuming this outlet exergy as an objective leads to higher exergetic efficiencies, 79% for domestic CGS and 96% to industrial as can be seen in table 5. However, the rate of exergy destruction is considerable, specially in domestic CGS, where $\dot{E}_d = 872kW$.

Table 4: Exergy balance of domestic (left) and industrial (right) CGS.

Exergy in	Qin+Flow	100%	100%
Exergy out	TE	20,11%	2,73%
	Flow	59,09%	93,03%
	Losses	0,08%	0,02%
Ex.Destroied	TE	4,31%	0,94%
	Boiler	16,41%	3,29%

Table 5: Exergetic analysis results.

	Domestic CGS		Industrial CGS	
	$\dot{E}_d$[kW]	ε[%]	$\dot{E}_d$[kW]	ε[%]
TE	182	82	0.82	0.21
Boiler	690	14	9	2.59
TE+Boiler	872	79	96	0.16

9. Conclusions

From the thermodynamic analysis, with all the constraints and boundary conditions that must be imposed, one concludes that recovering energy from pressure reduction stations is not as obvious as it seems. One of the main reasons is that the greater the difference between the inlet and outlet pressure, the higher the temperature drop and heating requirements. However, depending on the characteristics of the station and on the availability of heat sources nearby, there are many parameters that can be adjusted to make possible and attractive the energy production in a CGS. Despite having global efficiencies almost always below 100%, the main argument in favour of energy recovery at pressure reduction stations is based on economic reasons. If the boiler coupled to the HX works with the NG, the project may still be attractive because the cost of the kWh of NG is cheaper than the kWh of electricity. A domestic CGS can produce almost 7 GWh of electricity per year, which is equivalent to the electricity consumption of about 2.8 thousand typical Portuguese dwellings.

Considering that distribution companies pay €0.047 per kWh of electricity on this kind of pro-

duction and that the NG consumed costs nearly €0.019 per kWh, it can be said the the system is economically viable if:

$$\dot{W}(365 \times 24)C_{elect} - \dot{Q}(365 \times 24)C_{NG} > 0$$

$$\Rightarrow \frac{\dot{W}}{\dot{Q}} > \frac{C_{NG}}{C_{elect}}$$

$$\eta_{global} > 40\%$$

And as seen above, the global efficiency is always higher than 40%.

Acronyms

CGS	City Gate Station
CHP	Combined Heat and Power
EOS	Equation of State
HX	Heat Exchanger
NG	Natural Gas
PR	Pressure Ratio
TE	Turboexpander
VdW	Van der Waals

References

[1] Heinz P Bloch and Claire Soares. *Turboexpanders and Process Applications*. Gulf Professional Publishing, 2001.

[2] Bryan Lehman and Ernst Worrell. Electricity Production from Natural Gas Pressure Recovery Using Expansion Turbines. In *Proc. 2001 ACEEE Summer Study on Energy Efficiency in Industry*, volume 2, pages 24–27, 2001.

[3] CHP System Powers Electrabel Gas Distribution Center. Pipeline & Gas Journal, October 2002.

[4] Enbridge and FuelCell Energy Power Up World's First DFC-ERG Fuel Cell. http://www.marketwired.com/press-release/enbridge-inc-tsx-enb-913121.htm. Date accessed: 04-05-2018.

[5] Imran Nazir Unar, Aziza Aftab, Masroor Abro, et al. Estimation of Power Production Potential from Natural Gas Pressure Reduction Stations in Pakistan Using ASPEN HYSYS. *Mehran University Research Journal of Engineering & Technology*, 34(3):301, 2015.

[6] Natural Gas Infrastructures TPA Website. https://www.ign.ren.pt/en/. Date accessed: 05-05-2018.

[7] Rogério Duarte and Miguel Santos. Climatização Geosolar em Moura. 2012.

[8] EG Hammerschmidt. Formation of Gas Hydrates in Natural Gas Transmission Lines. *Industrial & Engineering Chemistry*, 26(8):851–855, 1934.

[9] Saeid Mokhatab and William A Poe. *Handbook of Natural Gas Transmission and Processing*. Gulf Professional Publishing, 2012.

[10] Michael J Moran, Howard N Shapiro, Daisie D Boettner, and Margaret B Bailey. *Fundamentals of Engineering Thermodynamics*. John Wiley & Sons, 2010.

[11] Kh Nasrifar and O Bolland. Prediction of Thermodynamic Properties of Natural Gas Mixtures Using 10 Equations of State Including a New Cubic Two-Constant Equation of State. *Journal of Petroleum Science and Engineering*, 51(3-4):253–266, 2006.

[12] Ulrich Setzmann and Wolfgang Wagner. A new equation of state and tables of thermodynamic properties for methane covering the range from the melting line to 625 k at pressures up to 100 mpa. *Journal of Physical and Chemical reference data*, 20(6):1061–1155, 1991.

[13] Abbas Zabihi and Majid Taghizadeh. Feasibility Study on Energy Recovery at Sari-Akand City Gate Station Using Turboexpander. *Journal of Natural Gas Science and Engineering*, 35:152–159, 2016.

[14] Navid Zehtabiyan Rezaie and Majid Saffar-Avval. Feasibility study of turbo expander installation in city gate station. In *Proceedings of the 25th International Conference on Efficiency, Cost, Optimization and Simulation of Energy Conversion Systems and Processes, Perugia, Italy*, volume 2629, page 47, 2012.

[15] Dossier de Imprensa - Tarifas e Preços para a Energia Elétrica em 2018. ERSE, 15-12-2017.